

Role of activated carbon surface chemistry in its photocatalytic activity and the generation of oxidant radicals under UV or solar radiation

I. Velo-Gala*, J.J. López-Peñalver, M. Sánchez-Polo, J. Rivera-Utrilla

Department of Inorganic Chemistry, Faculty of Science, University of Granada, 18071 Granada, Spain

ARTICLE INFO

Article history:

Received 10 December 2016
Received in revised form 1 February 2017
Accepted 2 February 2017
Available online 10 February 2017

Keywords:

UV radiation
Simulated solar radiation
Activated carbon
Photocatalysis
Radical species

ABSTRACT

We have studied the role that activated carbon surface chemistry plays in its photocatalytic activity under UV radiation and simulated solar radiation. In this study, we have used the commercial activated carbon Witco and five carbon samples obtained after its gamma radiation treatment, as this procedure allows the modification of the superficial chemistry of the carbon but not its physical properties. Sodium diatrizoate was used as a model compound for the degradation study. Its degraded percentage depends on the type of radiation and activated carbons used. To explain the carbon photocatalytic activity, we have demonstrated the formation of the electron hole as well as the formation of hydroxyl radicals and the superoxide anion in the UV/activated carbon and the Solar/activated carbon systems, and that the concentration of these oxidant species depends on the superficial chemistry of these materials. Moreover, the activated carbons, which have a smaller band gap allow higher concentrations of hydroxyl radicals, whilst those carbons with a larger band gap favour the formation of the superoxide anions. The degradation of the contaminant by UV/activated carbon and Solar/activated carbon systems has also been compared with the results obtained when the photocatalyst used is the traditional TiO₂. The activated carbon efficiency as a photocatalyst is higher than TiO₂ under UV radiation, which is due to the different concentrations of oxidant species produced in both systems.

© 2017 Elsevier B.V. All rights reserved.

1. Introduction

Treatment systems based on heterogeneous photocatalysis are one of the technologies to be considered in the treatment of contaminated water with organic compounds, which resist conventional processes [1,2]. In these systems, the radiation in the visible-ultraviolet range originates electronic activation in the

semiconductor material or catalyst. After its irradiation with a suitable wavelength, this material generates pairs of electron/holes, which are responsible for the formation of highly reactive species (hydroxyl radical, hydroperoxyl radical, superoxide anion, hydrogen peroxide, etc.) that will be involved in pollutant degradation [3–7]. In the processes of heterogeneous photocatalysis, the material used as a photocatalyst is essential because it determines the required wavelength of radiation to be applied to carry out the process. Therefore, the development of new materials that allow the use of sunlight is of great interest since most photocatalyst materials absorb UV light, which constitutes only a small fraction (3–5%) of the solar spectrum [8,9]. In addition, the use of traditional photocatalyst materials has other disadvantages, such as their complicated removal of the treated effluent and their high level of recombination of electron/hole pairs generated. Most of studies performed to solve these problems are based on the application of doping techniques of metal oxides, such as TiO₂, either by replacing a small fraction of the corresponding metal by another metal, such as iron, gold, copper, platinum and palladium, among others [10–14], or by replacing part of the oxygen of the photocatalyst by non-metallic elements, such as nitrogen, carbon and sulphur [10,11,14–16]. But

Abbreviations: AC, activated carbon; AOPs, advanced oxidation processes; Eg, band gap energy; DRS, diffuse reflectance spectra; DMSO, dimethyl sulfoxide; DNPH, 2,4 dinitrophenylhydrazine; DNPho, formaldehyde-2,4-dinitrophenylhydrazone; DTZ, sodium diatrizoate; EDTA, ethylenediaminetetraacetic acid; ESR, electron spin resonance; HPLC, high performance liquid chromatography; NF[−], nitroform anion; Solar/AC, simulated solar radiation and activated carbon system; TNM, tetrani-tromethane; UV, ultraviolet light; UV/AC, ultraviolet light and activated carbon system; W, Pristine activated carbon Witco; W-H[•], Witco carbon irradiated in the presence of H[•]; W-e[−]_{aq}, Witco carbon irradiated in the presence of e[−]_{eq}; W-OH, Witco carbon irradiated in the presence of OH[−]; W-0, Witco carbon irradiated in the presence of all radicals; W-a, Witco carbon irradiated in the air (without water); XPS, X-ray photoelectron spectroscopy.

* Corresponding author.

E-mail address: invega@ugr.es (I. Velo-Gala).

in all these cases the necessity to remove the photocatalyst from the effluent persists. To resolve this question photocatalysis immobilization on supports is proposed, with the use of porous materials being particularly interesting. Due to their high surface area and morphology, this type of support provides the advantage of the accommodation of the semiconductor material, without affecting its properties and the approximation of pollutants to the photocatalyst is facilitated [17–25]. Carbon materials have significantly improved the efficiency of the degradation process, which is largely attributed to their textural properties [22,26,27]. However, it has recently been shown that the improvement of the photocatalytic performance observed with some carbon materials exceeds their simple textural contribution. The complete degradation of contaminants in aqueous solution has been achieved by oxidation systems with UV radiation in the presence of activated carbon without the typical semiconductor materials [28–32]. In addition to this behaviour, it should be added that the consideration of some activated carbons as photocatalyst materials is correct as they maintain the role of preserving their physicochemical characteristics after the photocatalytic process and their reuse has demonstrated that these materials conserve their initial photoactivity after several cycles [30,33]. These results confirm that activated carbons have an important photocatalytic activity just under the action of UV radiation, so more studies are necessary to allow us to elucidate the action mechanisms and the properties of activated carbons that can explain this behaviour. F. Velasco et al. showed that the photoactivity of carbons was related by the combination of high porosity and the presence of photoreactive sites that favour the splitting of the exciton inside the pores. They pointed out that the incorporation of O-containing groups in carbon matrix decreased the photoconversion inside the pores [34]. Within this context, we think it is necessary to study in depth how influences the superficial chemistry of activated carbon in their photoactivity. Therefore, in our study, we have used a commercial activated carbon (Witco) and five new carbon samples obtained after its ionizing radiation treatment, because this procedure allows the modification of the superficial chemistry of the carbon but not its physical properties [35]. The present study represents a great breakthrough in the clarification of the origin of the photocatalytic activity of activated carbons. We directly analyse the phases that form the photocatalytic processes and the influence of the type of irradiation source used. Furthermore, it is expected that the chemistry of the activated carbon surface will have an important role in the processes of photo-oxidation. To analyse the photocatalytic activity, these activated carbon samples have been exposed to radiation with different energy sources, such as UV light and simulated solar radiation, the analysis of activated carbon photo-activity in this latter system being novel.

In other studies [34,36–42], the authors only detected the generation of hydroxyl radical in carbon materials using spin trapping and electron spin resonance (ESR) spectroscopy to detect radicals, measuring a spin trapping agent (5-diethoxyphosphoryl-5-methyl-1-pyrroline-N-oxide (DEPMPO) or 5,5-dimethylpyrroline-N-oxide (DMPO)). In our study, we propose a different method of mean to detect and quantify hydroxyl radicals and superoxide anion photogenerated. It is noteworthy that this is the first time that the quantification of reactive species concentrations produced by the photocatalytic activity of the activated carbons has been made by this methodology.

On the other hand, the efficiency of the UV radiation/activated carbon system (UV/AC system) and solar radiation/activated carbon system (Solar/AC system) is evaluated in terms of degradation of the sodium diatrizoate (DTZ) contrast media as the pollutant model. In our previous studies we obtained high degradation percentages of this compound by a photooxidation process in the presence of activated carbon under UV light but in the absence of a typical semi-

conductor [30] or using gamma radiation in presence of activated carbon [43]. In both studies, experimental data for DTZ adsorption kinetics on Witco activated carbon were obtained, and the results showed its low adsorption. This behaviour facilitates the study of the role of activated carbon surface chemistry in the photocatalytic activity of activated carbon.

With this background, the present work aims to demonstrate the photocatalytic behaviour of activated carbons in the presence of UV light and simulated solar radiation, by analysing the different reactions which form the photocatalytic processes such as the generation of electron/hole pairs and the formation of highly reactive species. For this purpose, our specific objectives were: (i) Propose a new methodology to detect and quantify hydroxyl radicals and superoxide anion photogenerated by the photocatalytic activity of the activated carbons; (ii) the study of the influence of the activated carbon amount in the photocatalysis processes with UV light and solar radiation; (iii) to evidence the existence of photogenerated positive holes in the materials; (iv) the quantification of the concentrations of superoxide and hydroxyl radicals formed by photocatalysis processes under UV light and simulated solar radiation; (v) to determine the role of dissolved oxygen in the medium in these photocatalytic processes; and (vi) the analysis of the influence of surface chemical properties of activated carbon in the formation of the different radical species quantified.

2. Experimental

2.1. Materials

All the chemical products used (sodium diatrizoate, formic acid, acetonitrile, methanol, hydrochloric acid, sodium chloride, tetranitromethane, dimethyl sulfoxide, ethylene diamine tetraacetic acid, atrazine) were high-purity analytical grade and supplied by Sigma-Aldrich, with the exception of Aeroxide TiO₂ P-25 (CAS-N° 13463-67-7), which was provided by Evonik Industries. All the solutions were prepared with ultra-pure water obtained using Milli-Q® equipment (Millipore). The original activated carbon used has the commercial name Witco. The rest of carbon samples used in this study are changes produced on Witco by applying gamma radiation under different conditions (Section 2.5).

2.2. Photoreactor of simulated solar radiation

The solar simulator used was a model 1500 Solarbox, Neurtek instruments brand, equipped with a Xenon lamp of 1500 W (PHILIPS XOP-15-OF, 1500 W), which supplies radiant energy in a spectral range from 280 to 825 nm (Fig. 1S). The photodegradation experiments were conducted in an irradiance of 450 W m⁻². The experiments were conducted in quartz tubes (wall-width of 3 mm, inner diameter of 22 mm and height of 220 mm) that have a 92% transmittance across the 200–2500 nm range, which were previously sealed to prevent the effect of evaporation. The activated carbon used was kept in suspension by a magnetic agitation system.

The photonic flux entering in the quartz tubes provided by the Xenon lamp, installed inside the solar radiation simulator, was determined by 2-nitrobenzaldehyde (o-NB) actinometry, adapting the method proposed by Willett and Hites [44]. Thus, 0.5 L solution of 2-nitrobenzaldehyde 2.5×10^{-3} M was prepared, using as solvent a mixing of ethanol in water 50:50. This solution was irradiated an irradiance of 450 W m⁻² and samples were drawn every 5 min. o-NB concentration was plotted as a function of irradiation time and the curve was fitted to first-order kinetics. The incident photon flow (I_0) was calculated through Eq. (1).

$$I_0 = \frac{d[\text{Act}]}{dt} \times \left(\frac{1}{\phi} \right) \times \left(\frac{1}{1 - 10^{-\epsilon \cdot b \cdot [\text{Act}]_0}} \right) \quad (1)$$

where Act is the o-NB concentration; ϕ , is the quantum yield of o-NB, $0.410 \pm 0.02 \text{ mol E}^{-1}$ across the 280–405 nm range [45]; ε , is the molar absorptivity, $128.6 \text{ L mol}^{-1} \text{ cm}^{-1}$; and b is the path length in cm of the light, 2.2 cm. Thus, the photon flow calculated was $2.95 \times 10^{-6} \text{ Einstein s}^{-1}$. The weighted average wavelength of our Xenon lamp was calculated by applying the procedure proposed by Natalia de la Cruz et al. [46], in the wavelength range of 290–400 nm, resulting to be 344 nm. Then, the energy of the photon is easily calculated from Planck's law, $5.78 \times 10^{-19} \text{ J photon}^{-1}$. The quartz tube has an area of 159.56 cm^2 and a volume of 135.47 cm^3 . Therefore, using all this data, the incident light flux in W m^{-2} was calculated, resulting 64.52 W m^{-2} .

2.3. Photoreactor of UV radiation

The photoreactor of UV radiation is equipped with a sample holder with a capacity for 6 quartz tubes (wall-width of 3 mm, inner diameter of 22 mm and height of 220 mm) that have a 92% transmittance for a wavelength of 254 nm. A low-pressure mercury lamp (Hg 253.70 nm, Fig. 1S) Heraeus Noblelight, model TNN 15/32 (15W), is placed in the centre of the sample holder to ensure uniform irradiation of the six quartz tubes. The photoreactor was filled with ultrapure water that surrounded the sample holder and mercury lamp and was maintained in continuous recirculation at a constant temperature ($298.0 \pm 0.2 \text{ K}$) using a Frigiterm ultrathermostat. The photoreactor was equipped with a magnetic agitation system for maintaining the solutions under constant agitation within the quartz tubes. The rate of energy irradiated by the lamp was determined by actinometry, using a solution of $5 \mu\text{M}$ atrazine as actinometer [47] and incident light flux was calculated through Eq. (1), obtaining light flux of 34.62 W m^{-2} , for the lamp used. For this purpose, the quantum yield of atrazine was considered to be 0.046 mol E^{-1} and the molar absorption coefficient to be $386 \text{ m}^2 \text{ mol}^{-1}$ at 254 nm wavelength [48].

2.4. Diatrizoate determination in aqueous solution

Diatrizoate concentration in aqueous solution was determined by reversed phase high performance liquid chromatography (HPLC) using a liquid chromatograph (Thermo-Fisher) equipped with a visible ultraviolet detector and auto-sampler with capacity for 120 vials. The chromatographic column was a Kinetex® C18 (2.6 μm particle size; $4.6 \times 150 \text{ mm}$). The mobile phase was 70% of 0.1% formic acid aqueous solution v/v and 30% of 0.1% formic acid acetonitrile solution in isocratic mode at flow of 0.45 mL min^{-1} ; detector wavelength was 254 nm and injection volume was $100 \mu\text{L}$.

2.5. Modification of activated carbon properties by gamma radiation treatment

We used the commercial activated carbon Witco (W) and five carbon samples obtained from the modification of the original by applying gamma radiation in different conditions as described in one of our previous papers [35]. The carbon samples were designated according to the radical present under gamma irradiation conditions (Table 1S). They are identified as follows: W, original Witco carbon; W-H[•], Witco carbon irradiated in the presence of H[•] radical; W-e^{-aq}, Witco carbon irradiated in the presence of e^{-aq}; W-•OH, Witco carbon irradiated in the presence of •OH radical; W-0, Witco carbon irradiated in the presence of all radicals; and W-a, Witco carbon irradiated in air (without water). The particle size of all carbon samples used was 0.25 mm.

2.6. Characterization of the activated carbon samples

All the activated carbon samples were texturally (N_2 adsorption at 77 K, CO_2 adsorption at 273 K) and chemically (elemental analysis, mineral material percentage, X-ray fluorescence (XRF), X-ray photoelectron spectroscopy (XPS) and the pH of point of zero charge (pHpzc)). Our research group previously reported the techniques used for the chemical and textural characterization of the carbon samples [35,49,50].

The main physical and chemical characteristics of the carbon samples are shown in Tables 2S–8S in Supplementary Information. Our results show that UV radiation produces no modification in carbon porosity (Table 4S). XPS results of surface chemistry of the W carbon series after UV radiation exposure for 3 and 15 min (Table 8S) indicated that the surface chemistry of the original W activated carbon underwent slight modifications, whereas differences were minimal on the irradiated W activated carbon samples after UV radiation exposure.

Photophysical properties of activated carbon were studied by means of diffuse reflectance spectroscopy (Fig. 2S). Diffuse reflectance spectra (DRS) of the powdered carbons were obtained by using a VARIAN CARY-5E double-beam UV–Vis and near infrared absorption spectrophotometer with wavelength measurements from 200 nm (6.20 eV) through 2000 nm (0.62 eV); the data were acquired at 1 nm intervals using a spectral bandwidth (SBW) of 2 nm for the whole spectrum with the exception of the infrared region, in which the SBW is not fixed. The Grating Switching Wavelength and Detector Switching Wavelength were 800 nm, and the Source Switching Wavelength was 310 nm. Baseline spectra were obtained from a sample of pressed barium sulfate powder. Samples were prepared by grinding 10 mg carbon with 100 mg barium sulfate [30]. Thus, based on the DRS, we studied the electronic properties of activated carbons according to the Kubelka–Munk theory. Wherefore, based on the DRS, we calculated the respective values of the band gap energy (E_g) (Table 7S) [51–53].

2.7. Diatrizoate adsorption kinetics on activated carbons

Experimental data for DTZ adsorption kinetics on activated carbons were obtained by placing 17 mg of activated carbon in contact with 100 mL of 25 mg L^{-1} DTZ solution at 298 K and pH 6.5. Samples were drawn at regular time intervals to determine the DTZ concentration for calculation of the amount adsorbed. The experimental conditions for the adsorption process were the same as for UV and solar radiation degradation in the presence of activated carbon. Samples were drawn at regular time intervals to a final time of 60 min. Samples were immediately filtered by Millipore disk filters (0.45 μm) to remove the activated carbon.

2.8. Photolysis of sodium diatrizoate

For the study of direct DTZ photolysis, 25 mg L^{-1} DTZ solutions were placed in the quartz tubes in the UV or solar photoreactors, depending on the type of radiation studied. These solutions were maintained under constant agitation during the entire experiment at a temperature of 298 K. Samples were drawn from each solution at regular time intervals for subsequent measurement of the DTZ concentration. The total time of the experiments was fixed at 15 min and 1 h for photolysis by UV radiation and simulated solar radiation, respectively.

2.9. Diatrizoate degradation by UV radiation or simulated solar radiation in the presence of photocatalyst materials

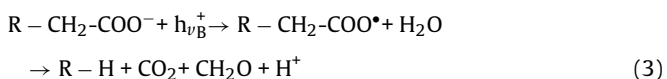
Experimental data for DTZ photodegradation (UV light and simulated solar radiation) in the presence of activated carbon were

obtained by the addition of 100 mL of 25 mg L⁻¹ solution of DTZ in the quartz tubes in the presence of 17 mg of activated carbon at pH 6.5 and 298 K under constant agitation. As in Section 2.8, samples were drawn at regular time intervals to follow DTZ degradation kinetics. Samples were immediately filtered by Millipore disk filters (0.45 µm) to remove the activated carbon.

To compare the results obtained in heterogeneous photocatalysis in the presence of activated carbons in the same conditions with the processes in which a traditional photocatalyst is used, the DTZ degradation in the presence of Aerioxide TiO₂ P-25 was studied.

2.10. Study of the generation of positive holes

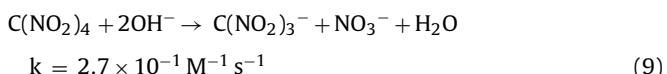
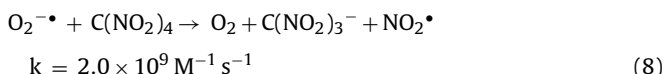
To study the degradation pathway of DTZ due to the generation of hydroxyl radicals, the experiments described in Section 2.9 were carried out but in the presence of ethylenediaminetetraacetic acid (EDTA) which acts as electron donor and therefore as positive hole scavenger [54–57] (Reactions (2)–(7)).



The concentration of EDTA used was 4 × 10⁻² M, adjusting the pH of the solution to a value of 7.5. It is important to control the medium pH value because we need EDTA to be in its deprotonated form and the repulsive electrostatic forces between the activated carbon and this compound not to occur, to favour its interaction with the positive hole photogenerated.

2.11. Quantification of superoxide anion concentration in the UV/AC and Solar/AC

The measurement of the concentration of the superoxide anion photogenerated was performed by quantifying the trinitromethane anion (NF⁻) formed by the reaction of superoxide anion with tetranitromethane (TNM) (Reaction (8)) [58]. The initial concentration used of TNM was 1 × 10⁻⁴ M. The concentration of the NF⁻ anion was measured with a spectrophotometer model Genesys 5 at a wavelength of 350 nm. The calibration curve was obtained by preparing different solutions of TNM at basic pH to hydrolyze the TNM and to produce NF⁻, given that 62% of initial concentration of TNM becomes in NF⁻ under these conditions [58] (Reaction (9)).

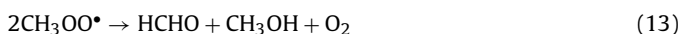
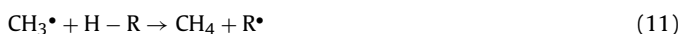


To compare the results obtained by UV/AC and Solar/AC systems with a traditional photocatalytic process with titanium dioxide, experiments were performed under these same conditions but substituting activated carbon for the same amount of titanium dioxide.

Furthermore, the influence of the amount of activated carbon on the superoxide radical generation was studied by adding different amounts of activated carbon W (35, 100, 170 and 235 mg L⁻¹) in a volume of 100 mL.

2.12. Quantification of hydroxyl radical in solution

The method used to quantify the concentration of hydroxyl radical generated in the different photocatalytic processes studied is based on its reaction with dimethyl sulfoxide (DMSO) compound ($k_{\text{OH}} = 4.5\text{--}7.1 \times 10^9 \text{ mol L}^{-1} \text{ s}^{-1}$) [59]. As a result of this reaction, formaldehyde is produced which reacts with 2,4-dinitrophenylhydrazine (DNPH) to form hydrazone (DNPHo) which is quantified by HPLC. To calculate the concentration of hydroxyl radical we must consider that one mole of formaldehyde is generated from two moles of hydroxyl radical after reacting with DMSO, according to Reactions (10)–(13) [59]:



The experimental conditions are an adaptation of the work of S. Dominguez [60] on the influence of the concentration of titanium dioxide in the generation of hydroxyl radical in a photocatalytic reactor LED. The study of the DMSO adsorption capacity of the six activated carbons was made, obtaining a maximum removal of 2% at two hours. We then carried out the heterogeneous photocatalysis experiments with different activated carbons in UV and simulated solar radiation reactors under the same photodegradation DTZ conditions (Section 2.9). A volume of 2 mL of filtered sample was added to 2.5 mL of H₃PO₄–NaH₂PO₄ buffer solution (pH 4.0), 0.2 mL of 6 mM DNPH solution dissolved in acetonitrile and 0.3 mL of ultra-pure water. This mixture was kept at room temperature for 60 min before being analysed by reversed HPLC using the same equipment described above (Section 2.4). The mobile phase used was a solution of methanol and Milli-Q water 60:40 v/v, with a flow of 0.35 mL min⁻¹. The detector wavelength was 355 nm and injection volume was 100 µL.

To compare the results obtained in UV/TiO₂ and Solar/TiO₂ systems, the same experiments were carried out, but substituting the activated carbon for the same amount of TiO₂ P-25 Aerioxide.

2.13. Study of the influence of dissolved oxygen in photocatalytic processes in the presence of activated carbon

The dissolved oxygen in the solution can react with the photogenerated electron to form the superoxide radical [61]. It is therefore necessary to study its role in the different systems considered in this study. So, we proceeded to remove the dissolved oxygen by bubbling nitrogen into the solution for 15 min before the experiment and during its development. The experimental conditions were as described in Section 2.8, with the original W activated carbon in the UV/AC system. The dissolved oxygen concentration was measured during the experiment with an oximeter DO 6+.

To verify if the oxygen content in the activated carbon structure participates in the photocatalytic process, the same experiment was repeated, but with the activated carbon W previously dried in an oven at 383 K.

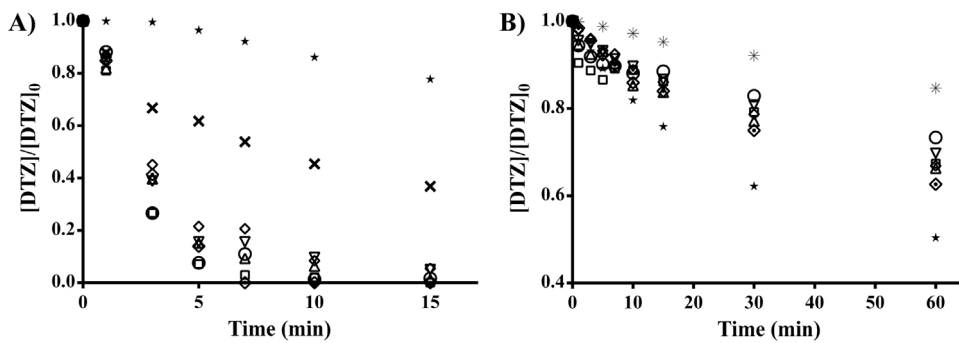


Fig. 1. DTZ degradation by UV light and simulated solar radiation. A) UV radiation: (x), direct photolysis; (★), UV/TiO₂ system; UV/AC system with activated carbons W (○), W-H⁺ (□), W-e⁻_{aq} (△), W-·OH (▽), W-0 (◊) y W-a (◇). B) Simulated solar radiation: (★), direct photolysis; (x), Solar/TiO₂ system; Solar/AC system with activated carbons W (○), W-H⁺ (□), W-e⁻_{aq} (△), W-·OH (▽), W-0 (◊). [DTZ]₀ = 25 mg L⁻¹; W_{AC} = W_{TiO₂} = 17 mg; λ = 254 nm; pH = 6.5; T = 298 K.

3. Results and discussion

3.1. Influence of the type of radiation in the heterogeneous photocatalysis process using activated carbon

First of all, the variations in the concentration of the contaminant sodium diatrizoate by the action of UV light and simulated solar radiation were determined, both in the absence and presence of activated carbon or TiO₂ as photocatalyst materials. Our results (Fig. 1 and Table 9S) show that direct photolysis of DTZ is greater when UV radiation is used, since the degradation percentage of 63.20% is achieved compared to 15.27% obtained when simulated solar radiation is applied. This is due to the absorption spectrum of the DTZ (Fig. 1S) because its absorbance is maximum in the range of 200–270 nm, where the emission wavelength of the low-pressure mercury lamp is (λ = 253.70 nm).

The emission spectrum of the Xenon lamp of the solar photoreactor (Fig. 1S) shows that the overlap between the emission spectrum of the xenon lamp and the absorption spectrum of DTZ is minimum. This is the reason for the low percentage of DTZ degradation by direct simulated solar radiation. In addition, the results for DTZ adsorption on activated carbons (Table 10S) show that is insignificant for a treatment time of 60 min, which justifies the suitability of these compound for evaluating only the photocatalytic activity of activated carbon samples.

Furthermore, our results show that these activated carbons have a photoactive behaviour, whether UV radiation or simulated solar radiation are used, because the percentage of DTZ removed is higher than the degradation rate obtained by direct photolysis. We observe that the increased effect in DTZ degradation, due to the presence of activated carbon, is greater under UV radiation.

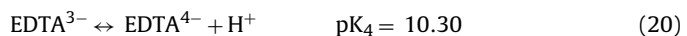
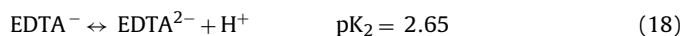
In addition, photocatalysis experiments were performed with Aerioxide TiO₂ P-25 in order to compare the results between activated carbon samples and a conventional photocatalyst as TiO₂. The observed results varied depending on the type of incident radiation. Thus, the DTZ degradation was higher in the Solar/TiO₂ system than in Solar/AC systems (Fig. 1, Table 9S), a similar effect was observed by other authors [62]. This behaviour is due to the significant difference in illumination intensity created by the solar light, 64.52 W m⁻², against 34.62 W m⁻² of photoreactor of UV radiation. If these results are compared with the experiments in the absence of AC, we can observe that the Solar/AC systems have a higher degradation percentage. However, when the degradation process is carried out with UV radiation, the degradation rates obtained by UV/AC systems are much higher than those obtained with the UV/TiO₂ system. Thus, the presence of TiO₂ in the solution increases the flux of absorbed photons [63–65], which generates more electron-hole pairs, which increases the opportunity for

electron-hole recombination. All of this, contributes to decrease the relative number of the photoinduced carriers taking part in the reaction with DTZ, on the surface of TiO₂ particles, and for this reason the percentage of DTZ degradation is even lower than that obtained by direct photolysis.

In order to deepen and justify these results, and considering our previous research showing the photoactive behaviour of activated carbons [30], in the following sections we analyse the photogenerated species in the systems described above depending on the type of material and radiation.

3.2. Study of the positive holes photogenerated in the UV/AC and Solar/AC systems

In the photocatalysis process (Reactions (14)–(16)), positive holes are generated after the promotion of electrons from the valence band to the conduction band. The positive holes are responsible for the generation of hydroxyl radicals (Reaction (16)), hence the importance of their study. For this reason, we carried out photocatalysis experiments in the presence of EDTA as it reacts with photogenerated positive holes in the material (Reactions (2)–(7)) [54–57], preventing the Reaction (16) occurring and, therefore, the formation of hydroxyl radicals. Experiments were carried out at pH = 7.5 since with this pH EDTA is in its deprotonated form, equilibria showed in Reactions (17)–(20) [66]. Moreover, the final pH is equal than the initial pH.



Initially, the photogenerated positive holes oxidize the EDTA³⁻ acetate group to form CO₂ and CH₂O, but the latter also reacts by removing electrons (Reactions (4)–(7)) and therefore EDTA is a scavenger of superoxide anion formations, which is the another way of oxidizing species generation in photocatalytic processes [56,67]. The results obtained (Fig. 2) show that EDTA inhibits the photocatalytic effect of the activated carbons. This effect is more pronounced in the UV/AC system, where the degradation percentages of DTZ are lower than those obtained by direct photolysis. This behaviour can be explained considering that, without photocatalyst action and given the zero adsorption removal of DTZ on

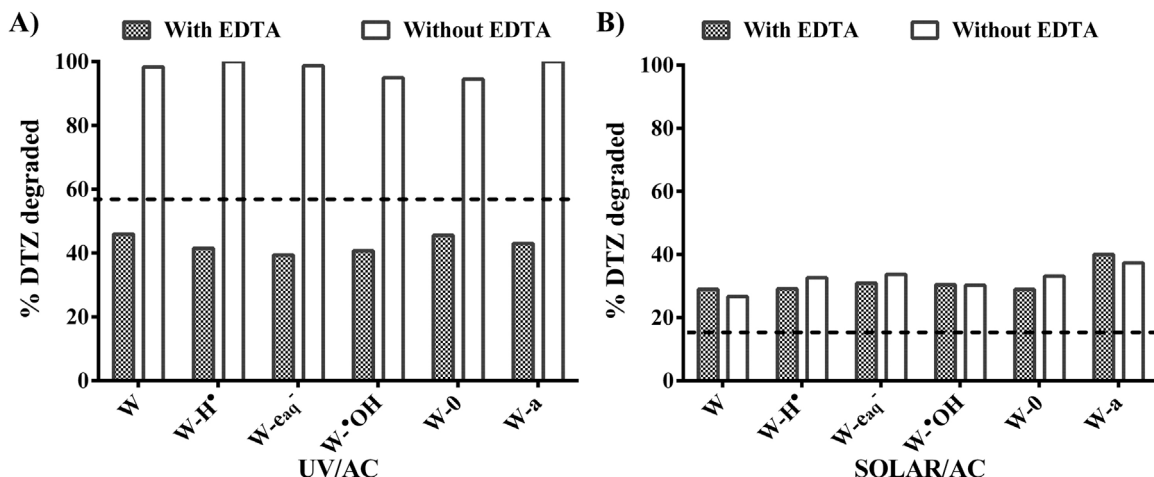


Fig. 2. EDTA influence in DTZ degradation by UV/AC and Solar/AC systems. A) UV/AC system; B) Solar/AC system. (----), % degradation of DTZ by direct photolysis. $[DTZ]_0 = 25 \text{ mg L}^{-1}$; $[EDTA]_0 = 4.0 \times 10^{-2} \text{ M}$; $W_{AC} = 17 \text{ mg}$; $pH = 7.5$; $T = 298 \text{ K}$.

these materials (Table 10S), the activated carbon will have the simple effect of shielding between the incident UV radiation and DTZ, thus hindering degradation by direct photolysis.

However, the results are completely different if the incident energy is simulated solar radiation, in which case the presence of $EDTA^{3-}$ does not influence the DTZ degradation (Fig. 2B). The reason for this different behaviour is that the type of incident radiation controls the reaction of EDTA with photogenerated positive holes and electrons. UV radiation catalyses both the reaction in which formaldehyde is consumed to give formic acid, as well as its reaction to form CO_2 (Reactions (3)–(7)) [54–57]. The reactions, which consume the degradation products from $EDTA^{3-}$, are favoured meaning a higher removal of photogenerated positive holes and electrons [56]. On the other hand, the fraction of incident radiation with sufficient energy to catalyse the reactions of degradation products formed after the reaction between $EDTA^{3-}$ and photogenerated positive holes or electrons, is only 3–5% when simulated solar radiation is used. This causes the efficiency of EDTA as an inhibitor of the process in the Solar/AC system to decrease drastically. Therefore, there is no difference between the percentage of DTZ degradation in the both the presence and absence of EDTA with the Solar/AC system.

In order to interpret the adsorption behaviour of EDTA onto the activated carbon surface, it is necessary to consider the pH_{pzc} value of activated carbons (Table 5S). Activated carbons $W-OH$, $W-a$, $W-e_{aq}$ and W have pH_{pzc} value higher than the pH study ($pH = 7.5$) and therefore activated carbon surface carries a positive charge. This situation favours attractive electrostatic interactions between adsorbate and adsorbent. Carbon $W-0$ has no charge due to its pH_{pzc} value is proximity at the study pH, whereas carbon $W-H$ has a net negative charge and favour repulsive electrostatic interactions between adsorbate and adsorbent. But the results shown in Fig. 2 indicate that there are no significant differences in the behaviour of the six activated carbon, both in UV/AC system and in Solar/AC system. These results suggest that besides the electrostatic interactions between adsorbate and adsorbent there must be another mechanism involved. Anoop Krishnan et al. suggest that activated carbons act as anion exchangers through an inner sphere complex formation mechanism by a ligand exchange process. In such a mechanism, the surface OH groups of activated carbon would be exchanged with $EDTA^{3-}$ in the aqueous phase as follows [68]. This behaviour justifies the results obtained for carbon $W-H^{\bullet}$.

3.3. Study of superoxide anion formation in the UV/AC and Solar/AC systems

In the previous section we described the formation of positive holes in the UV/AC and Solar/AC systems. The generation of these positive holes lead to the formation of an electron (Reaction (14)), which may react with oxygen to form a superoxide anion (Reaction (15)). In our previous studies [30], we found that the photocatalytic behaviour of AC depends on the amount of carbon present in the system. Therefore, we have studied how the amount of AC influences the photogeneration of superoxide anions, measuring their concentration based on the amount of the activated carbon W used.

Fig. 3 shows how the photogeneration of the superoxide anion changes depending on the treatment time, and the amount of AC, in UV/AC (Fig. 3A) and Solar/AC (Fig. 3B) systems. In the case of the UV/AC system, the experimental data are adjusted to a pseudo-first order kinetic and we calculated the values of the rate constants of the superoxide anion photogeneration: $3.45 \times 10^{-3} \text{ M}^{-1} \text{ s}^{-1}$ with 35 mg L^{-1} of AC, $7.19 \times 10^{-3} \text{ M}^{-1} \text{ s}^{-1}$ with 100 mg L^{-1} of AC, $1.87 \times 10^{-2} \text{ M}^{-1} \text{ s}^{-1}$ with 170 mg L^{-1} of AC, and $9.81 \times 10^{-3} \text{ M}^{-1} \text{ s}^{-1}$ with 235 mg L^{-1} of AC. These values show that the rate constants increase exponentially up to 170 mg L^{-1} of AC and from this value on, the formation rate of superoxide anion also decreases exponentially (Fig. 3S). This behaviour conforms to a growing exponential equation when $[AC] \leq 170 \text{ mg L}^{-1}$ and decreases exponentially when $[AC]$ is $> 170 \text{ mg L}^{-1}$ (Eq. (21)):

$$r_{O_2^- \text{ generation}} = 2.007 \cdot 10^{-3} \times e^{1.31 \cdot 10^{-2} \times [AC]} \quad \text{where } [AC] \leq 170 \text{ mg L}^{-1} \quad (21)$$

$$r_{O_2^- \text{ generation}} = 1.003 \cdot 10^{-1} \times e^{-9.89 \cdot 10^{-3} \times [AC]} \quad \text{where } [AC] > 170 \text{ mg L}^{-1}$$

where $r_{O_2^- \text{ generation}}$ is the rate of the superoxide anion generation expressed in $\text{M}^{-1} \text{ s}^{-1}$ and $[AC]$ is the AC concentration provided in mg L^{-1} .

In the Solar/AC system, the superoxide anion concentration reaches its maximum values quickly when $[AC]$ is $\geq 100 \text{ mg L}^{-1}$, stabilizing it in short reaction times (Fig. 3B). We calculate the response surfaces, which relate how the concentration of the superoxide anion changes dependent on the reaction time and the amount of AC in the system (Fig. 4S). These response surfaces can determine the AC concentration, which produces the maximum concentration of superoxide anion; 138 mg L^{-1} in the UV/AC system and 167 mg L^{-1} in the Solar/AC system. Therefore, we consider that the optimum concentration of AC is 170 mg L^{-1} , as it allows the maximum concentration of superoxide anion in the Solar/AC

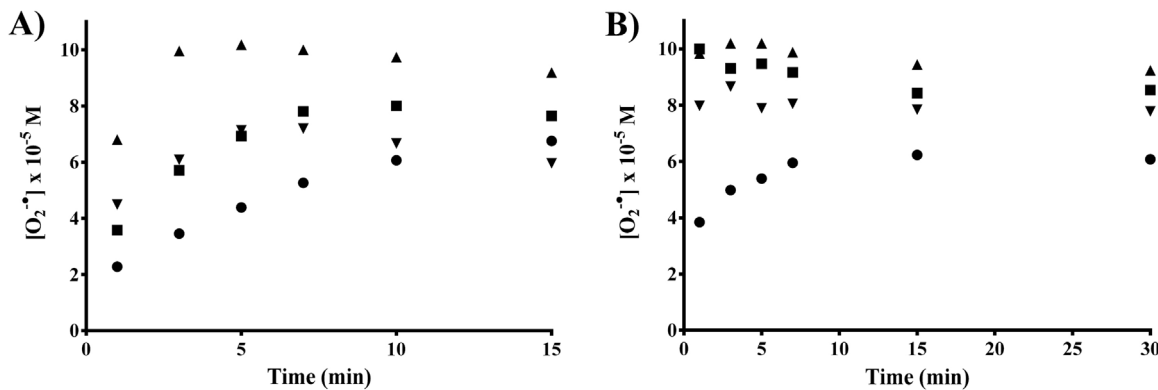


Fig. 3. Concentration of photogenerated superoxide anion depending on the amount of activated carbon added to the system. A) UV/AC system; B) Solar/AC system. Amount of activated carbon (mg L^{-1}): (●), 35; (■), 100; (▲), 170; (▼), 235. AC = W; $\text{pH} = 6.5$; $T = 298 \text{ K}$.

system and this value is in the range where its maximum concentration is reached in the UV/AC system (Fig. 3A). Furthermore, the experimental results show that once the photogeneration of superoxide anions has reached its maximum value, the concentration remains constant for reaction times higher than 10 min (Fig. 3 and Fig. 4S). This behaviour is different when we use TiO_2 as a photocatalyst (Fig. 5S), because the concentration of superoxide anion decreases slightly for times of less than 5 min in the UV/ TiO_2 system and then remains constant during the reaction time. This value is lower in a 71.05% of the superoxide anion concentration obtained with UV/AC system. With the simulated solar radiation application (Solar/ TiO_2 system), we observed that the superoxide radical concentration reaches its maximum value ($5.83 \times 10^{-5} \text{ M}$) for reaction times between 0 and 5 min, and then decreases until it is stable at a concentration of $3.34 \times 10^{-5} \text{ M}$. This value is significantly lower than that obtained in the Solar/AC system ($1.02 \times 10^{-4} \text{ M}$) (Fig. 4S). This different behaviour can be attributed to the higher surface area of activated carbon W, $815 \text{ m}^2 \text{ g}^{-1}$ (Table 3S), compared to $50 \text{ m}^2 \text{ g}^{-1}$ of aeroxide TiO_2 P-25 [69], because this favours the contact between the dissolved oxygen in the medium and the AC surface, and this situation is necessary for the generation reaction of the superoxide anion (Reaction (15)). Furthermore, the presence of chemisorbed oxygen on the surface of AC (Table 7S) helps this reaction to occur to a greater extent. All of this results in a higher concentration of superoxide anion generated in the UV/AC system.

3.4. Study of the hydroxyl radical generation in the UV/AC and Solar/AC systems

In the light of these results in which the formation of the superoxide anion depends on the AC amount added to the system, we studied the effect on the formation of hydroxyl radical for the UV and solar systems. The results (Fig. 4) show that the hydroxyl radical concentration is independent of the AC amount in the Solar/AC system (Fig. 4B). The maximum mean concentration of hydroxyl radical was $5.36 \times 10^{-5} \text{ M}$. Moreover, the hydroxyl radical concentration increases with time and with the quantity of AC in the UV/AC system. The data $[^\bullet\text{OH}]$ vs time was adjusted to a kinetics of pseudo-first order (Fig. 4A), the photogeneration rate constant of the hydroxyl being $1.12 \times 10^{-2} \text{ M}^{-1} \text{ s}^{-1}$ with 35 mg L^{-1} of AC, $2.01 \times 10^{-2} \text{ M}^{-1} \text{ s}^{-1}$ with 100 mg L^{-1} of AC, $3.33 \times 10^{-2} \text{ M}^{-1} \text{ s}^{-1}$ with 170 mg L^{-1} of AC and $4.23 \times 10^{-2} \text{ M}^{-1} \text{ s}^{-1}$ with 235 mg L^{-1} of AC. These values of photogeneration rate of the hydroxyl radical show that there is a linear dependence with the concentration of AC (Fig. 6S) in the concentration range of AC studied, $30\text{--}235 \text{ mg L}^{-1}$.

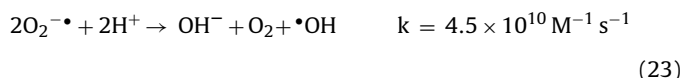
AC. This behaviour fits a linear equation (Eq. (22)) with a correlation coefficient of $R^2 = 0.9981$:

$$r_{^\bullet\text{OH}_{\text{generation}}} = 5.596 \times 10^{-3} + 1.579 \times 10^{-4}[\text{AC}]. \quad (22)$$

where, $r_{^\bullet\text{OH}_{\text{generation}}}$ is the rate of hydroxyl radical generation in $\text{M}^{-1} \text{ s}^{-1}$ and $[\text{AC}]$ is the concentration of activated carbon present in the system in mg L^{-1} .

We determined the amount of AC which generated the maximum concentration of hydroxyl radical by the surface response methodology (Fig. 7S) and it was 156 mg L^{-1} AC in the UV/AC system and 191 mg L^{-1} in the Solar/AC system.

If we compare how the concentration of superoxide anion changes with the concentration of hydroxyl radical and the amount of AC (Fig. 5A), we can observe that the concentrations of hydroxyl radical and the superoxide anion increase together to a fixed amount of AC. But when the OH radical concentration is higher than $8.82 \times 10^{-5} \text{ M}$, the superoxide anion concentration decreases as the OH radical increases. Moreover, if we compare how the rate of formation of both radicals changes depending on the current amount of AC (Fig. 5B), we can observe that the formation of both oxidant species is favoured with small amounts of AC because the formation rate of both increases. However, the formation rate of the superoxide anion decreases sharply when the AC amounts are $>170 \text{ mg L}^{-1}$, while the formation rate of hydroxyl radical continues to increase. This behaviour could be attributed to the formation of hydroxyl radical (Reaction (16)) leading to the formation of H^+ on the AC surface, and an increase in its concentration favouring the occurrence of the Reaction (23) in a further extension, and that the equilibrium shown in the Reaction (24) is moved towards the left. This makes the Reactions (25) and (26) take place and this would justify the decrease in concentration of superoxide anion and the increased concentration $^\bullet\text{OH}$ radical. Whereas the formation rate of the hydroxyl radical is higher than the superoxide anion, the decrease in the superoxide anion concentration may also occur because both species react with one another (Reaction (27)) [70].



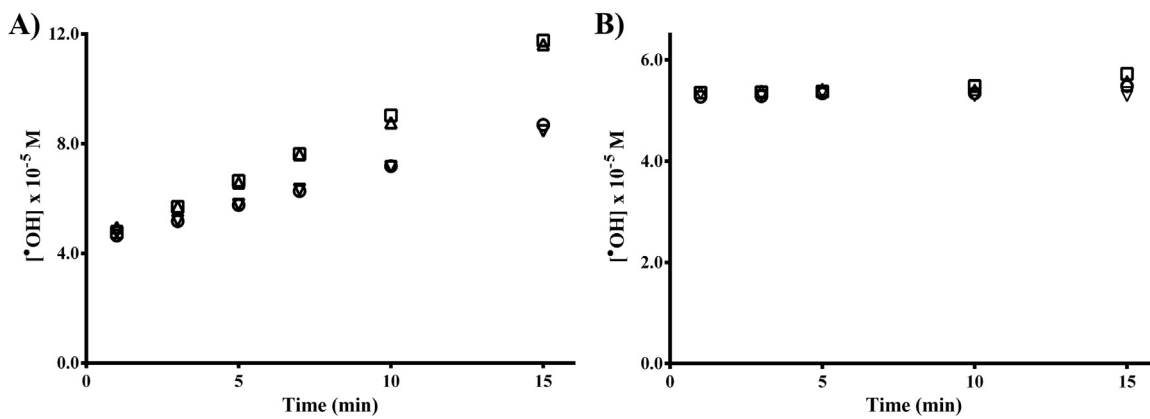


Fig. 4. Hydroxyl radical concentration depending on the amount of activated carbon added to the system. A) UV/AC system; B) Solar/AC system. Amount of activated carbon (mg L^{-1}): (○), 35; (□), 100; (△), 170; (▽), 235. AC = W; pH = 6.5; T = 298 K.

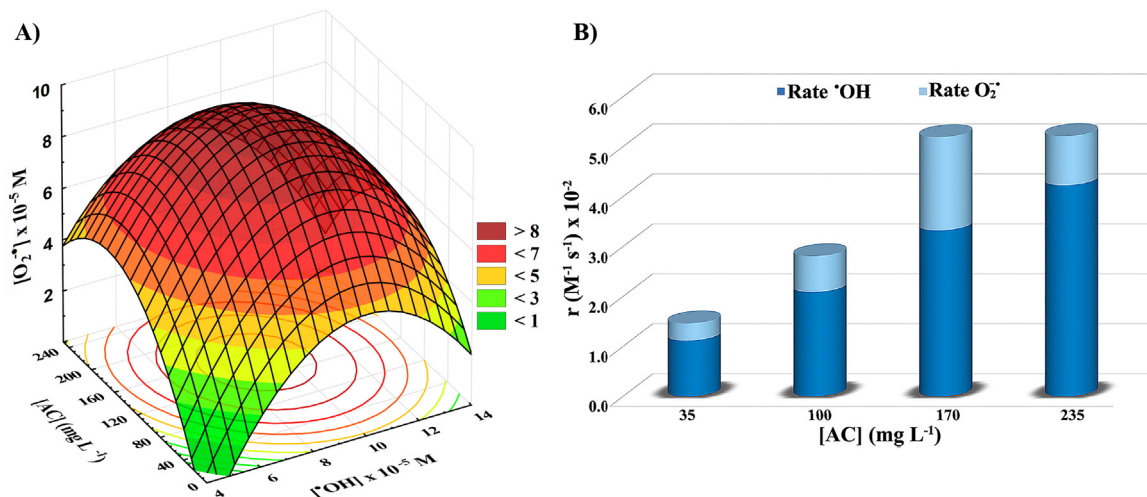


Fig. 5. Variations of the concentrations and formation rates of the superoxide anion and the hydroxyl radical in the UV/AC system according to the quantity of AC. A) Variation of the superoxide anion concentration depending on the hydroxyl radical concentration and the quantity of AC; B) Variation in the formation rate of the superoxide anion and the hydroxyl radical depending on the quantity of AC. pH = 6.5; T = 298 K.

3.5. Role of oxygen as the promoter of the heterogeneous photocatalysis process

Oxygen plays a key role in the photocatalytic process to such an extent that its withdrawal from the medium implies full/partial inhibition of photocatalytic activity of the photocatalyst materials [71]. This is because its presence in the medium prevents Reaction (15), thus favouring the recombination of the electron/positive hole pairs generated.

In our previous studies, we have shown that the absence of dissolved oxygen in the medium originated the reduction of the degradation percentages of the model contaminant to similar levels to those obtained by direct photolysis levels, indicating that activated carbon ceased acting as a photoactive material [30]. In order to analyse these first results, we studied how the formation of superoxide anion changed its concentration in the medium in the absence of dissolved oxygen and by the removal of the chemisorbed oxygen in the material (Fig. 8S).

The data show that there is a maximum reduction of 12.45% ($t = 5.0 \text{ min}$) in the concentrations of superoxide anion when carbon W was used without chemisorbed oxygen (carbon W was previously dried in the heater). This indicates that the chemisorbed oxygen on the material participates in the generation of superoxide anion and therefore in the photocatalytic process. But the dissolved oxygen in water is what further determines the forma-

tion of superoxide anion as in its absence, the concentration of this oxidant species is reduced by an average of 86.13%. Therefore, for the activated carbon to show its photoactivity, it is necessary for the oxygen to be dissolved in the solution or for the oxygen to be chemisorbed on the carbon surface.

3.6. Influence of AC surface chemistry in the photo-generation of radical species in the UV/AC and Solar/AC systems

Once the different behaviour of AC under UV and solar radiations had been established, we studied the influence of the AC surface chemical nature. To do this, we modified the surface chemistry of the activated carbon Witco using gamma radiation, as this procedure changes its surface chemistry (Table 5S–7S) but not its physical characteristics (Table 3S) [35]. We obtained five new activated carbons (Table 1S) and we calculated the photogeneration of hydroxyl radicals and superoxide anion for each material (Fig. 6). We then compared these results with those produced by the Aerioxide TiO₂ P-25.

The concentrations of the superoxide anion and the hydroxyl radical show that there are significant differences between the application of UV radiation or simulated solar radiation, and that they differ from one AC sample to another and with Aerioxide TiO₂ P-25. In the case of TiO₂ we observed that the higher concentration of hydroxyl radical is reached by Solar/TiO₂ system (Fig. 6C). This

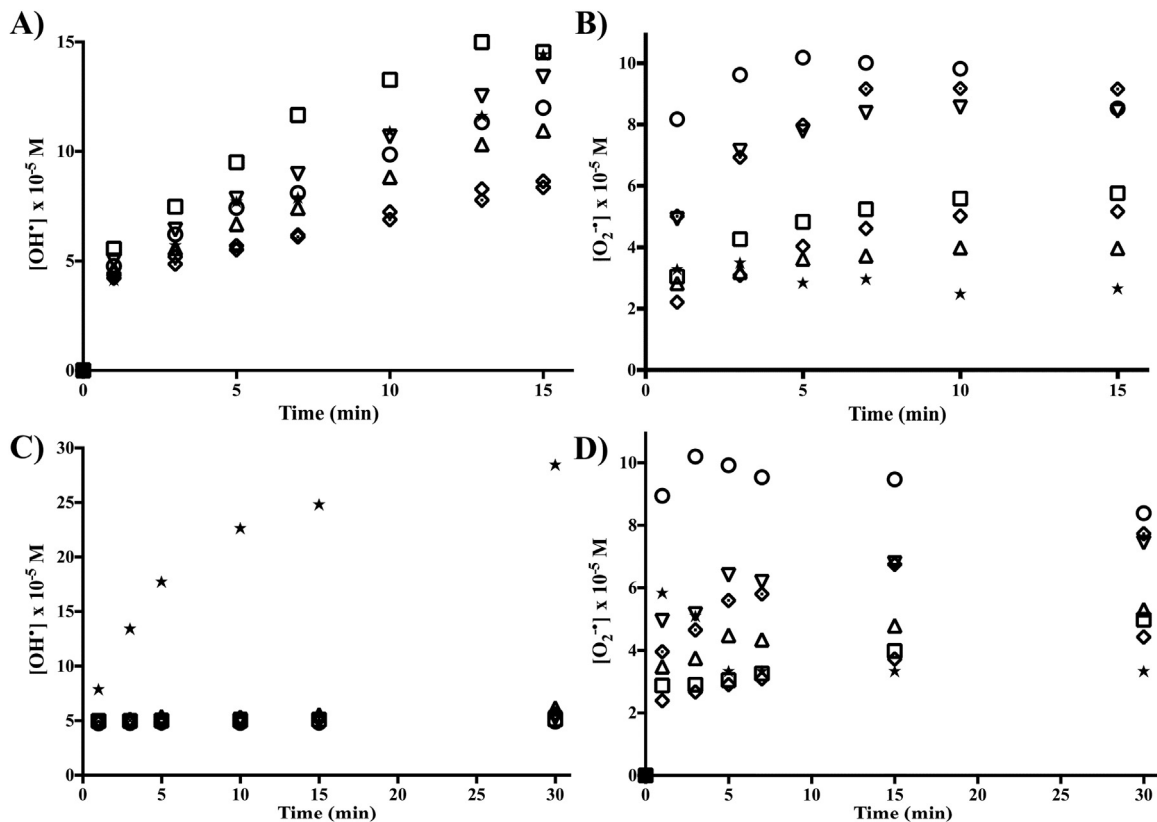


Fig. 6. Photogeneration of hydroxyl radicals and superoxide anion in the UV/TiO₂, UV/AC, Solar/TiO₂ and Solar/AC systems with irradiated carbons and Aerioxide TiO₂ P-25. A) Photogeneration of hydroxyl radicals by UV irradiation; B) photogeneration of superoxide anion by UV irradiation; C) photogeneration of hydroxyl radicals by simulated solar radiation; D) photogeneration of superoxide anion by simulated solar radiation. (★), Aerioxide TiO₂ P-25; (○), AC W pristine; (□), W-H[•]; (△), W-e^{-aq}; (▽), W-OH; (△), W-O; (▽), W-a. AC = TiO₂ = 17 mg; pH = 6.5; T = 298 K.

result proves those shown in Section 3.1, in which the DTZ degradation was the highest for this system, being higher than that obtained by the Solar/AC systems. On the other hand, the amounts of superoxide anion generated by TiO₂ P-25 are less than those generated by the different AC samples, both when UV radiation and simulated solar radiation are applied. Moreover, we observed a very different behaviour of AC behaviour under the action of UV radiation and simulated solar radiation, indicating that there must be some AC property that determines the effectiveness of the photogeneration process. Since the different AC samples used have the same textural properties but different surface chemistry, this latter property may be responsible for the different behaviour observed in terms of photogenerated species. Therefore, we analysed if there is some correlation between the surface chemistry of the AC samples and the concentrations of superoxide anions and hydroxyl radicals for each one, using Multi-factor analysis of variance (ANOVA) and Spearman's rank correlation coefficients. The results by ANOVA (Tables 11S–18S) show that the concentration of photogenerated hydroxyl radicals and superoxide anions depends on the surface chemistry of the AC samples. Thus, the results for the non-parametric statistical test Spearman's rank correlation coefficients (Table 19S) show that: i) the concentration of photogenerated hydroxyl radicals in the UV/AC system increases when the lactone and anhydrides surface groups are higher but the inverse occurs when the carboxyl surface groups, water or chemisorbed oxygen and physisorbed water increases; ii) for the superoxide anion, we observed that an increase of the physisorbed water involves an increase of its concentration in the UV/AC system; iii) in the Solar/AC system, the hydroxyl radical concentration increases with the increase of the concentration of carboxyl groups but the concentration of superoxide anion decreases as the quinone groups and carboxyl groups sur-

face increases, with the lactone and anhydride groups growing, and physisorbed water; and iv) in both the AC/UV system and the Solar/AC system, the concentration of superoxide anion increased by the shake-up makes the π-π* transitions in the aromatic rings, suggesting that the aromatic ring system may help the stabilization of the photogenerated electron. Moreover, the surface oxygen groups contribute to stabilizing the electrons generated on the AC surface [72].

The analysis of our results confirms that the behaviour of the UV/AC and Solar/AC systems differs between themselves, which may be attributed to the nature of the transitions involved in the incident radiation adsorption process by the AC. Thus, when UV radiation is used the π-π* transitions would be involved in the radiation absorption process [73–76], while in the case of simulated solar radiation, while the emission of spectrum lamp used is in the range of 300–800 nm, its absorption is related to the σ-π* transitions, because these transitions correspond to λ ≥ 320 nm, or with the activation of chromophore groups present on the carbon surface [77,78].

The other hand, amorphous carbon consists of an inhomogeneous mixture of sp² and sp³ sites. The sp³ sites have a wide gap, between the σ and σ* states. The sp² sites have a variable gap, which depends on the configuration of each sp² cluster and involve π-π* transition. The optical properties are determined by the π states on the sp² sites [79]. The absorption of radiation by carbon causes π-π* transition and as result electron-hole pairs are formed [73], responsible for the formation of radicals determined in the systems radiation/AC. Moreover, the band gap is controlled by the ordering and distortions of π states on sp² sites, and the sp² ordering depends on the sp³ fraction. Therefore, we studied the relationship between the concentration of the hydroxyl radicals, the superox-

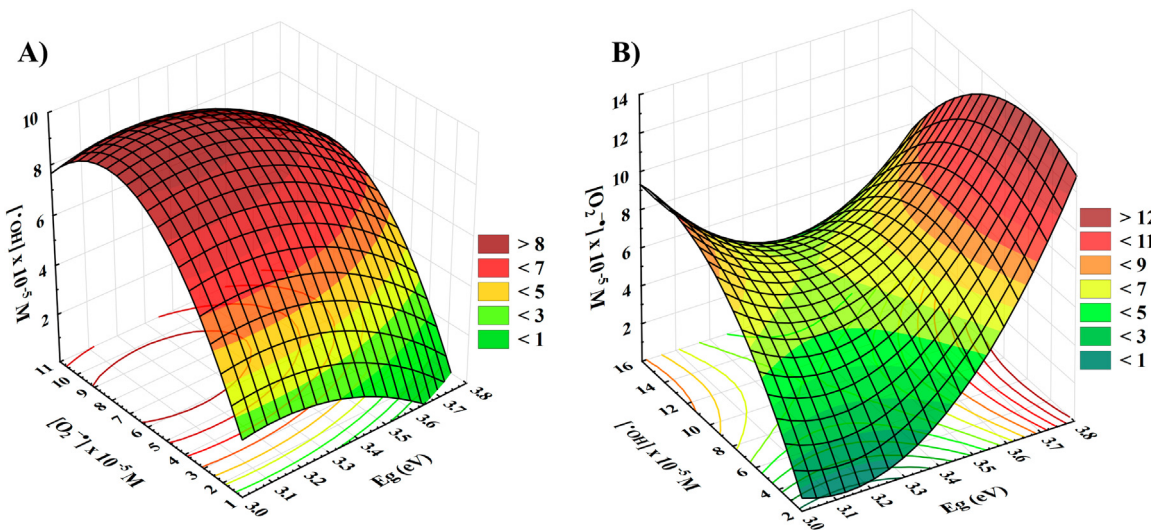


Fig. 7. Variation in the concentration of photoinduced oxidant species based on the value of the energy band gap. A) Variation of the hydroxyl radical concentration in function of the superoxide anions concentration and the Eg value. B) Variation of the superoxide anion concentration in function of the hydroxyl radical concentration and the Eg value.

ide anions and the band gap of each AC sample used (the values of band gap, Eg, of the AC used were determined in our previous study [35]). When we represent the variation of the concentration of the hydroxyl radical as a function of the concentration of superoxide anion and the value of Eg, (Fig. 7A), we observe that the AC sample with the lowest Eg value, favours the hydroxyl radical formation, whilst the formation of superoxide anions is favoured when the material has a higher Eg value (Fig. 7B). These results allow us to establish for the first time the relationship between the value of band gap of activated carbon and the predominant photogenerated species in the medium. Thus, the band gap of activated carbons would condition that the medium predominate one oxidant agent or another. This result is of great importance since depending on the behaviour of the pollutant against hydroxyl radical or superoxide anion, we should choose an activated carbon that had a band gap lower or higher.

3.7. Relation between photogenerated oxidant species and the degradation of the model contaminant in the studied systems

The DTZ degradation rates obtained when UV/AC and Solar/AC systems are used are much higher than those obtained when only UV or simulated solar radiation are used (Table 9S). This behaviour can be explained if we consider: First, that DTZ adsorption on Witco activated carbon is very low [30,35,43] and second, that AC acts as a photocatalyst generating hydroxyl radicals which contribute to DTZ degradation and therefore, radiation + AC systems are more efficient than when only the radiation is used. When we compared the behaviour of activated carbons versus the traditional photocatalyst TiO₂, we observed different behaviours, with the best results when the activated carbon is applied under UV light instead of titanium dioxide. In the Solar/TiO₂ system, the percentage of degraded DTZ is higher than when the Solar/AC system is used, because the hydroxyl radical concentration determined in the Solar/TiO₂ system is much higher than that obtained with all the ACs under simulated solar radiation (Fig. 6). Moreover, comparing the percentages of DTZ degradation with their corresponding concentrations of hydroxyl radical in both systems, we observed how the results of degradation vary with the same concentration of hydroxyl radical (Fig. 9S), with radiation/AC systems being higher. This is due to the electrostatic attractive interactions between DTZ and AC, as we demonstrated in our previous study [43]. These

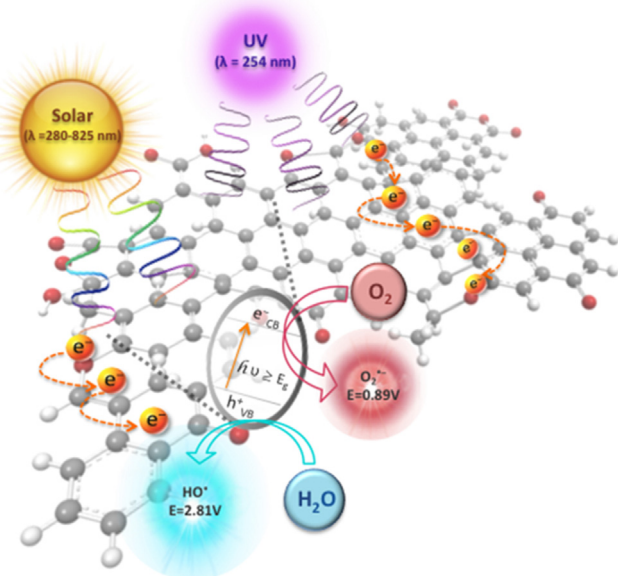


Fig. 8. Photocatalytic mechanisms proposed for the catalytic activity of activated carbon under simulated solar radiation or UV radiation.

attractive interactions between the AC surface and DTZ facilitate the reaction between the contaminant and the photogenerated radical, so that for the same concentration of radicals the process is more efficient when AC is used.

3.8. Photocatalytic mechanisms of activated carbon under simulated solar radiation or UV radiation

The results obtained suggest that the activated carbons have catalytic activity, when they are irradiated by light with an energy higher than their band gap. Upon irradiation, electron (e⁻_{CB}) and electron hole (h⁺_{VB}) pairs will first form (Reaction (28)) on the surface of activated carbon (Fig. 8). In the presence of H₂O the electron hole can form hydroxyl radicals (Reaction (29)). On the other side, the photogenerated electron reacts with oxygen molecule to form superoxide anion (Reaction (30)), which can react with the water molecule and trigger the formation of oxidizing radical species

(Reactions (31)–(32)) that will interact with the pollutant, contributing to its degradation. Furthermore, in the case of activated carbon the presence of adsorbed oxygen avoids recombination of the electron with the positive hole, allowing reaction between the adsorbed oxygen molecule and the photogenerated electron (Reaction (33)), increasing the he oxidizing species in the medium. This last process can encourage interaction between the water molecule and the free hole and increasing the effectiveness of the photocatalytic process.



4. Conclusions

The experimental results show that the activated carbons used have photocatalytic behaviour regardless of whether the incident light is UV or simulated solar radiation. However, the contaminant degradation processes are different. With simulated solar radiation, the percentage of DTZ degradation was higher when titanium dioxide was used. Conversely, if the incident radiation is UV light, the degradation rates obtained are much greater when the activated carbon is the photocatalyst, reaching DTZ removal values above 94% in all cases.

The determination of the hydroxyl radical and superoxide anion in the UV/AC and Solar/AC systems demonstrates that the AC acts as a photocatalyst material and the photoinduced reactive species are responsible for the highest degradation values of the contaminant, which are much higher than those obtained when only radiation is used.

The photogenerated concentrations of superoxide anion and hydroxyl radical depend on the surface chemistry of the activated carbons. We observed that the formation of hydroxyl radicals is favoured when Eg values are lower, whilst superoxide anion concentration is favoured in those activated carbons with higher Eg values.

We demonstrated that dissolved oxygen in the solution plays an important role in the photoactive behaviour of the activated carbons, so that its removal from the solution favours the recombination of electron-hole pairs, preventing the formation of superoxide anions and therefore, the generation of hydroxyl radicals. We also demonstrated that the presence of chemisorbed oxygen on the activated carbon surface promotes the formation of radical species, so carbons with a high concentration of surface oxygen could result in materials with a higher photoactive character.

We show that radiation/AC systems are more efficient in the degradation of the contaminant model than the radiation/TiO₂ systems, because attractive electrostatic interactions between the activated carbon surface and the contaminant promote the degradation reaction by photogenerated hydroxyl radicals.

Finally, it should be noted that the photocatalyst role of activated carbons is favoured by the presence of ester/anhydrid groups, as well as a higher percentage of carbon atoms with sp² hybridization.

Acknowledgements

The authors are grateful for the financial support provided by the Junta de Andalucía (grant number RNM7522) and the Spanish

Ministry of Science and Innovation (grant number CTQ2016-80978-C2-1-R).

Appendix A. Supplementary data

Supplementary data associated with this article can be found, in the online version, at <http://dx.doi.org/10.1016/j.apcatb.2017.02.028>.

References

- [1] J. Rivera-Utrilla, M. Sánchez-Polo, M.Á. Ferro-García, G. Prados-Joya, R. Ocampo-Pérez, Pharmaceuticals as emerging contaminants and their removal from water. A review, *Chemosphere* 93 (2013) 1268–1287.
- [2] M.N. Chong, B. Jin, C.W.K. Chow, C. Saint, Recent developments in photocatalytic water treatment technology: a review, *Water Res.* 44 (2010) 2997–3027.
- [3] S. Ahmed, M.G. Rasul, W.N. Martens, R. Brown, M.A. Hashib, Heterogeneous photocatalytic degradation of phenols in wastewater: a review on current status and developments, *Desalination* 261 (2010) 3–18.
- [4] U.G. Akpan, B.H. Hameed, Parameters affecting the photocatalytic degradation of dyes using TiO₂-based photocatalysts: a review, *J. Hazard. Mater.* 170 (2009) 520–529.
- [5] P. Fernández-Ibáñez, M.I. Polo-López, S. Malato, S. Wadhwa, J.W.J. Hamilton, P.S.M. Dunlop, R. D'sa, E. Magee, K. O'shea, D.D. Dionysiou, J.A. Byrne, Solar photocatalytic disinfection of water using titanium dioxide graphene composites, *Chem. Eng. J.* 261 (2015) 36–44.
- [6] U.I. Gaya, A.H. Abdullah, Heterogeneous photocatalytic degradation of organic contaminants over titanium dioxide: a review of fundamentals, progress and problems, *J. Photochem. Photobiol. C* 9 (2008) 1–12.
- [7] A. Özkan, M.H. Özkan, R. Gürkan, M. Akçay, M. Sökmen, Photocatalytic degradation of a textile azo dye, *Sirius Gelb GC* on TiO₂ or Ag-TiO₂ particles in the absence and presence of UV irradiation: the effects of some inorganic anions on the photocatalysis, *J. Photochem. Photobiol. A* 163 (2004) 29–35.
- [8] A. Primo, H. García, Chapter 6 – solar photocatalysis for environment remediation, in: S.L. Suib (Ed.), *New and Future Developments in Catalysis*, Elsevier, Amsterdam, 2013, pp. 145–165.
- [9] X. Zong, L. Wang, Ion-exchangeable semiconductor materials for visible light-induced photocatalysis, *J. Photochem. Photobiol. C* 18 (2014) 32–49.
- [10] M. Pelaez, N.T. Nolan, S.C. Pillai, M.K. Seery, P. Falaras, A.G. Kontos, P.S.M. Dunlop, J.W.J. Hamilton, J.A. Byrne, K. O'Shea, M.H. Entezari, D.D. Dionysiou, A review on the visible light active titanium dioxide photocatalysts for environmental applications, *Appl. Catal. B* 125 (2012) 331–349.
- [11] E. Grabowska, J. Reszczyńska, A. Zaleska, Mechanism of phenol photodegradation in the presence of pure and modified-TiO₂: A review, *Water Res.* 46 (2012) 5453–5471.
- [12] A. Ayati, A. Ahmadpour, F.F. Bamoharram, B. Tanhaei, M. Mänttäri, M. Sillanpää, A review on catalytic applications of Au/TiO₂ nanoparticles in the removal of water pollutant, *Chemosphere* 107 (2014) 163–174.
- [13] M.A. Rauf, M.A. Meetani, S. Hisaindee, An overview on the photocatalytic degradation of azo dyes in the presence of TiO₂ doped with selective transition metals, *Desalination* 276 (2011) 13–27.
- [14] C.M. Teh, A.R. Mohamed, Roles of titanium dioxide and ion-doped titanium dioxide on photocatalytic degradation of organic pollutants (phenolic compounds and dyes) in aqueous solutions: a review, *J. Alloys Compd.* 509 (2011) 1648–1660.
- [15] R. Marschall, L. Wang, Non-metal doping of transition metal oxides for visible-light photocatalysis, *Catal. Today* 225 (2014) 111–135.
- [16] L.G. Devi, R. Kavitha, A review on non metal ion doped titania for the photocatalytic degradation of organic pollutants under UV/solar light: role of photogenerated charge carrier dynamics in enhancing the activity, *Appl. Catal. B* 140–141 (2013) 559–587.
- [17] M.V. Phanikrishna Sharma, V. Durga Kumari, M. Subrahmanyam, TiO₂ supported over porous silica photocatalysts for pesticide degradation using solar light: part 2. Silica prepared using acrylic acid emulsion, *J. Hazard. Mater.* 175 (2010) 1101–1105.
- [18] Z. Liu, Z. Liu, T. Cui, J. Li, J. Zhang, T. Chen, X. Wang, X. Liang, Photocatalysis of two-dimensional honeycomb-like ZnO nanowalls on zeolite, *Chem. Eng. J.* 235 (2014) 257–263.
- [19] M.V. Phanikrishna Sharma, G. Sadanandam, A. Ratnamala, V. Durga Kumari, M. Subrahmanyam, An efficient and novel porous nanosilica supported TiO₂ photocatalyst for pesticide degradation using solar light, *J. Hazard. Mater.* 171 (2009) 626–633.
- [20] K. Venkata Subba Rao, A. Rachel, M. Subrahmanyam, P. Boule, Immobilization of TiO₂ on pumice stone for the photocatalytic degradation of dyes and dye industry pollutants, *Appl. Catal. B* 46 (2003) 77–85.
- [21] W. Wei, C. Yu, Q. Zhao, X. Qian, G. Li, Y. Wan, Synergy effect in photodegradation of contaminants from water using ordered mesoporous carbon-based titania catalyst, *Appl. Catal. B* 146 (2014) 151–161.
- [22] G. Li Puma, A. Bono, D. Krishnaiah, J.G. Collin, Preparation of titanium dioxide photocatalyst loaded onto activated carbon support using chemical vapor deposition: a review paper, *J. Hazard. Mater.* 157 (2008) 209–219.

- [23] A.Y. Shan, T.I.M. Ghazi, S.A. Rashid, Immobilisation of titanium dioxide onto supporting materials in heterogeneous photocatalysis: a review, *Appl. Catal. A* 389 (2010) 1–8.
- [24] J.L. Figueiredo, M.F.R. Pereira, The role of surface chemistry in catalysis with carbons, *Catal. Today* 150 (2010) 2–7.
- [25] F. Rodríguez-Reinoso, The role of carbon materials in heterogeneous catalysis, *Carbon* 36 (1998) 159–175.
- [26] R. Leary, A. Westwood, Carbonaceous nanomaterials for the enhancement of TiO₂ photocatalysis, *Carbon* 49 (2011) 741–772.
- [27] T.-T. Lim, P.-S. Yap, M. Srinivasan, A.G. Fane, TiO₂/AC composites for synergistic adsorption–photocatalysis processes: present challenges and further developments for water treatment and reclamation, *Crit. Rev. Env. Sci. Technol.* 41 (2011) 1173–1230.
- [28] L.F. Velasco, J.B. Parra, C.O. Ania, Role of activated carbon features on the photocatalytic degradation of phenol, *Appl. Surf. Sci.* 256 (2010) 5254–5258.
- [29] L.F. Velasco, I.M. Fonseca, J.B. Parra, J.C. Lima, C.O. Ania, Photochemical behaviour of activated carbons under UV irradiation, *Carbon* 50 (2012) 249–258.
- [30] I. Velo-Gala, J.J. López-Péñalver, M. Sánchez-Polo, J. Rivera-Utrilla, Activated carbon as photocatalyst of reactions in aqueous phase, *Appl. Catal. B* 142–143 (2013) 694–704.
- [31] C.O. Ania, L.F. Velasco, T. Valdés-Solís, Chapter 17 – photochemical behavior of carbon adsorbents, in: J.M.D. Tascón (Ed.), *Novel Carbon Adsorbents*, Elsevier, Oxford, 2012, pp. 521–547.
- [32] M. Haro, L.F. Velasco, C.O. Ania, Carbon-mediated photoinduced reactions as a key factor in the photocatalytic performance of C/TiO₂, *Catal. Sci. Technol.* 2 (2012) 2264–2272.
- [33] L.F. Velasco, R.J. Carmona, J. Matos, C.O. Ania, Performance of activated carbons in consecutive phenol photooxidation cycles, *Carbon* 73 (2014) 206–215.
- [34] L.F. Velasco, A. Gomis-Berenguer, J.C. Lima, C.O. Ania, Tuning the surface chemistry of nanoporous carbons for enhanced nanoconfined photochemical activity, *Chem. Cat. Chem.* 7 (2015) 3012–3019.
- [35] I. Velo-Gala, J.J. López-Péñalver, M. Sánchez-Polo, J. Rivera-Utrilla, Surface modifications of activated carbon by gamma irradiation, *Carbon* 67 (2014) 236–249.
- [36] A. Gomis-Berenguer, M. Seredysh, J. Iniesta, J.C. Lima, T.J. Bandosz, C.O. Ania, Sulfur-mediated photochemical energy harvesting in nanoporous carbons, *Carbon* 104 (2016) 253–259.
- [37] L.F. Velasco, V. Maurino, E. Laurenti, I.M. Fonseca, J.C. Lima, C.O. Ania, Photoinduced reactions occurring on activated carbons. A combined photooxidation and ESR study, *Appl. Catal. A* 452 (2013) 1–8.
- [38] L.F. Velasco, V. Maurino, E. Laurenti, C. Ania, Light-induced generation of radicals on semiconductor-free carbon photocatalysts, *Appl. Catal. A* 453 (2013) 310–315.
- [39] L. Wang, X. Cheng, Z. Wang, C. Ma, Y. Qin, Investigation on Fe-Co binary metal oxides supported on activated semi-coke for NO reduction by CO, *Appl. Catal. B* 201 (2017) 636–651.
- [40] X. Li, X. Liu, C. Qi, C. Lin, Activation of periodate by granular activated carbon for acid orange 7 decolorization, *J. Taiwan Inst. Chem. E* 68 (2016) 211–217.
- [41] A. Tyagi, T. Matsumoto, T. Kato, H. Yoshida, Direct C–H bond activation of ethers and successive C–C bond formation with benzene by a bifunctional palladium–titania photocatalyst, *Catal. Sci. Technol.* 6 (2016) 4577–4583.
- [42] F. Cataldo, M.V. Putz, O. Ursini, G. Angelini, Surface modification of activated carbon fabric with ozone. Part 3: Thermochemical aspects and electron spin resonance, *Fueler. Nanotub. Car.* N 24 (2016) 406–413.
- [43] I. Velo-Gala, J.J. López-Péñalver, M. Sánchez-Polo, J. Rivera-Utrilla, Role of activated carbon on micropollutants degradation by ionizing radiation, *Carbon* 67 (2014) 288–299.
- [44] K.L. Willett, R.A. Hites, Chemical actinometry: using o-Nitrobenzaldehyde to measure light intensity in photochemical experiments, *J. Chem. Educ.* 77 (2000) 900–902.
- [45] E.S. Galbavy, K. Ram, C. Anastasio, 2-Nitrobenzaldehyde as a chemical actinometer for solution and ice photochemistry, *J. Photochem. Photobiol. A* 209 (2010) 186–192.
- [46] N. De la Cruz, V. Romero, R.F. Dantas, P. Marco, B. Bayarri, J. Giménez, S. Esplugas, o-Nitrobenzaldehyde actinometry in the presence of suspended TiO₂ for photocatalytic reactors, *Catal. Today* 209 (2013) 209–214.
- [47] S. Canonica, L. Meunier, U. von Gunten, Phototransformation of selected pharmaceuticals during UV treatment of drinking water, *Water Res.* 42 (2008) 121–128.
- [48] G. Prados-Joya, M. Sánchez-Polo, J. Rivera-Utrilla, M. Ferro-garcía, Photodegradation of the antibiotics nitroimidazoles in aqueous solution by ultraviolet radiation, *Water Res.* 45 (2011) 393–403.
- [49] M. Sánchez-Polo, J. Rivera-Utrilla, Effect of the ozone–carbon reaction on the catalytic activity of activated carbon during the degradation of 1,3,6-naphthalenetrisulphonic acid with ozone, *Carbon* 41 (2003) 303–307.
- [50] J. Rivera-Utrilla, M. Sánchez-Polo, Ozonation of naphthalenesulphonic acid in the aqueous phase in the presence of basic activated carbons, *Langmuir* 20 (2004) 9217–9222.
- [51] P. Kubelka, New contributions to the optics of intensely light-scattering materials, *J. Opt. Soc. Am.* 38 (1948) 448–457.
- [52] P. Kubelka, F. Munk, Ein Beitrag zur optik der farbanstriche, *Z. Tech. Phys. (Leipzig)* 12 (1931) 593–601.
- [53] R. López, R. Gómez, Band-gap energy estimation from diffuse reflectance measurements on sol-gel and commercial TiO₂: a comparative study, *J. Sol. Gel Sci. Technol.* 61 (2012) 1–7.
- [54] X. Li, Y. Fan, W. Jin, Y. Huang, N. Xu, J. Shi, Effect of EDTA on preparation of Pd membranes by photocatalytic deposition, *Desalination* 192 (2006) 117–124.
- [55] T. Chen, G. Wu, Z. Feng, G. Hu, W. Su, P. Ying, C. Li, In situ FT-IR study of photocatalytic decomposition of formic acid to hydrogen on Pt/TiO₂ catalyst, *Chin. J. Catal.* 29 (2008) 105–107.
- [56] E.-C. Su, B.-S. Huang, C.-C. Liu, M.-Y. Wey, Photocatalytic conversion of simulated EDTA wastewater to hydrogen by pH-resistant Pt/TiO₂-activated carbon photocatalysts, *Renew. Energy* 75 (2015) 266–271.
- [57] S. Yuh-Fan, W. Guan-Bo, K. Dave-Ta Fu, C. Meei-Ling, S. Yang-Hsin, Photoelectrocatalytic degradation of the antibiotic sulfamethoxazole using TiO₂/Ti photoanode, *Appl. Catal. B* 186 (2016) 184–192.
- [58] R. Flynt, A. Leitzke, G. Mark, E. Mvula, E. Reisz, R. Schick, C. von Sonntag, Determination of •OH, O₂^{•-}, and hydroperoxide yields in ozone reactions in aqueous solution, *J. Phys. Chem. B* 107 (2003) 7242–7253.
- [59] C. Tai, J.F. Peng, J.F. Liu, G.B. Jiang, H. Zou, Determination of hydroxyl radicals in advanced oxidation processes with dimethyl sulfoxide trapping and liquid chromatography, *Anal. Chim. Acta* 527 (2004) 73–80.
- [60] S. Dominguez, P. Ribao, M.J. Rivero, I. Ortiz, Influence of radiation and TiO₂ concentration on the hydroxyl radicals generation in a photocatalytic LED reactor. Application to dodecylbenzenesulfonate degradation, *Appl. Catal. B* 178 (2015) 165–169.
- [61] A.J. Hoffman, E.R. Caraway, M.R. Hoffmann, Photocatalytic production of H₂O₂ and organic peroxides on quantum-sized semiconductor colloids, *Environ. Sci. Technol.* 28 (1994) 776–785.
- [62] R. Kralchevska, M. Milanova, M. Tsvetkov, D. Dimitrov, D. Todorovsky, Influence of gamma-irradiation on the photocatalytic activity of Degussa P25 TiO₂, *J. Mater. Sci.* 47 (2012) 4936–4945.
- [63] A. Tolosana-Moranchel, J.A. Casas, J. Carbo, M. Faraldo, A. Bahamonde, Influence of TiO₂ optical parameters in a slurry photocatalytic reactor: kinetic modelling, *Appl. Catal. B* 200 (2017) 164–173.
- [64] B. Bayarri, J. Giménez, D. Curcó, S. Esplugas, Direct evaluation of the absorbed photon flow in a photocatalytic reactor by an actinometric method, *Chem. Eng. J.* 200–202 (2012) 158–167.
- [65] C. -y. Wang, J. Rabani, D.W. Bahnemann, J.K. Dohrmann, Photonic efficiency and quantum yield of formaldehyde formation from methanol in the presence of various TiO₂ photocatalysts, *J. Photochem. Photobiol. A* 148 (2002) 169–176.
- [66] E.P. Serjeant, Boyd Dempsey, International Union of Pure and Applied Chemistry. Commission on Electrochemical Data., Ionisation Constants of Organic Acids in Aqueous Solution, Pergamon Press Oxford, New York, 1979.
- [67] T.H. Madden, A.K. Datye, M. Fulton, M.R. Prairie, S.A. Majumdar, B.M. Stange, Oxidation of metal-EDTA complexes by TiO₂ photocatalysis, *Environ. Sci. Technol.* 31 (1997) 3475–3481.
- [68] K. Anoop Krishnan, K.G. Sreejalakshmi, S. Varghese, T.S. Anirudhan, Removal of EDTA from aqueous solutions using activated carbon prepared from rubber wood sawdust: kinetic and equilibrium modeling, *Clean Soil Air Water* 38 (2010) 361–369.
- [69] M. Faycal Atitar, A.A. Ismail, S.A. Al-Sayari, D. Bahnemann, D. Afanasev, A.V. Emeline, Mesoporous TiO₂ nanocrystals as efficient photocatalysts: impact of calcination temperature and phase transformation on photocatalytic performance, *Chem. Eng. J.* 264 (2015) 417–424.
- [70] G.V. Buxton, C.L. Greenstock, W.P. Helman, A.B. Ross, Critical Review of rate constants for reactions of hydrated electrons, hydrogen atoms and hydroxyl radicals (OH/O[•]) in aqueous solution, *J. Phys. Chem. Ref. Data* 17 (1988) 2593–2600.
- [71] D. Zhang, R. Qiu, L. Song, B. Eric, Y. Mo, X. Huang, Role of oxygen active species in the photocatalytic degradation of phenol using polymer sensitized TiO₂ under visible light irradiation, *J. Hazard. Mater.* 163 (2009) 843–847.
- [72] E.A. Voudrias, R.A. Larson, V.L. Snoeyink, Importance of surface free radicals in the reactivity of granular activated carbon under water treatment conditions, *Carbon* 25 (1987) 503–515.
- [73] A.D. Modestov, J. Gun, O. Lev, Graphite photoelectrochemistry study of glassy carbon, carbon-fiber and carbon-black electrodes in aqueous electrolytes by photocurrent response, *Surf. Sci.* 417 (1998) 311–322.
- [74] D. Dasgupta, F. Demichelis, C.F. Pirri, A. Tagliaferro, π bands and gap states from optical absorption and electron-spin-resonance studies on amorphous carbon and amorphous hydrogenated carbon films, *Phys. Rev. B: Condens. Matter* 43 (1991) 2131–2135.
- [75] M. Godard, E. Dartois, Photoluminescence of hydrogenated amorphous carbons-Wavelength-dependent yield and implications for the extended red emission, *Astron. Astrophys.* 519 (2010) A39.
- [76] D. Pan, J. Zhang, Z. Li, C. Wu, X. Yan, M. Wu, Observation of pH-, solvent-, spin-, and excitation-dependent blue photoluminescence from carbon nanoparticles, *Chem. Commun.* 46 (2010) 3681–3683.
- [77] L.F. Velasco, J.C. Lima, C. Ania, Visible-light photochemical activity of nanoporous carbons under monochromatic light, *Angew. Chem. Int. Ed.* 53 (2014) 4146–4148.
- [78] G. Eda, Y.Y. Lin, C. Mattevi, H. Yamaguchi, H.A. Chen, I.S. Chen, C.W. Chen, M. Chhowalla, Blue photoluminescence from chemically derived graphene oxide, *Adv. Mater.* 22 (2010) 505–509.
- [79] J. Robertson, E.P. O'Reilly, Electronic and atomic structure of amorphous carbon, *Phys. Rev. B: Condens. Matter* 35 (1987) 2946–2957.